

## Synthesis and kinetics of titanium silicides from photovoltaic industry waste and steelmaking slag for silicon and titanium recovery

Chen, Zhiyuan; You, Yuliu; Morita, Kazuki

**DOI**

[10.1021/acssuschemeng.8b00919](https://doi.org/10.1021/acssuschemeng.8b00919)

**Publication date**

2018

**Document Version**

Final published version

**Published in**

ACS Sustainable Chemistry and Engineering

**Citation (APA)**

Chen, Z., You, Y., & Morita, K. (2018). Synthesis and kinetics of titanium silicides from photovoltaic industry waste and steelmaking slag for silicon and titanium recovery. *ACS Sustainable Chemistry and Engineering*, 6(5), 7078-7085. <https://doi.org/10.1021/acssuschemeng.8b00919>

**Important note**

To cite this publication, please use the final published version (if applicable). Please check the document version above.

**Copyright**

Other than for strictly personal use, it is not permitted to download, forward or distribute the text or part of it, without the consent of the author(s) and/or copyright holder(s), unless the work is under an open content license such as Creative Commons.

**Takedown policy**

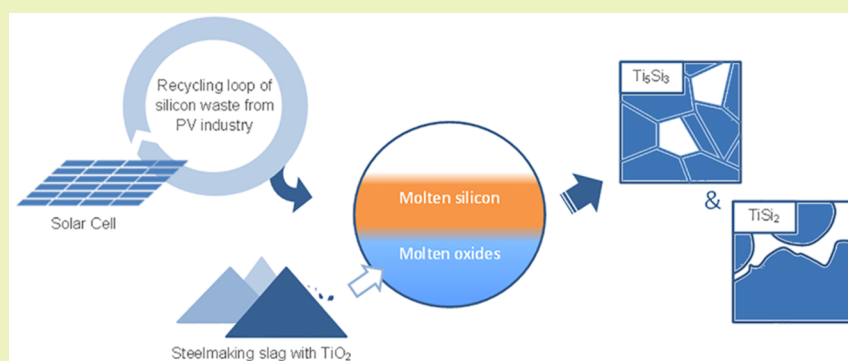
Please contact us and provide details if you believe this document breaches copyrights. We will remove access to the work immediately and investigate your claim.

# Synthesis and Kinetics of Titanium Silicides from Photovoltaic Industry Waste and Steelmaking Slag for Silicon and Titanium Recovery

Zhiyuan Chen,<sup>\*,†,‡,§</sup> Yuliu You,<sup>†,‡</sup> and Kazuki Morita<sup>†</sup>

<sup>†</sup>Department of Materials Engineering, Engineering, Building #4, Graduate School of Engineering, The University of Tokyo, 7-3-1 Hongo, Bunkyo-ku, Tokyo 113-8656, Japan

<sup>‡</sup>Department of Materials Science and Engineering, Block H, Building 34, Delft University of Technology, Mekelweg 2, 2628 CD Delft, The Netherlands



**ABSTRACT:** The increasing amount of silicon waste generated from the rapid developing photovoltaic industry calls for an economical silicon recycling process. The present work proposes a facile process with which silicon waste and ironmaking slag containing  $\text{TiO}_2$  were used as raw materials to produce titanium silicides, a promising high added value material. The process was experimentally investigated in lab scale. The result shows that a high  $\text{CaO}/\text{SiO}_2$  ratio in slag promotes the reaction.  $\text{TiSi}_2$  and  $\text{Ti}_5\text{Si}_3$  could be synthesized as principal products within 0.5 and 3 h with  $\text{CaO}/\text{SiO}_2 = 1.31$  in mass, respectively.  $\text{CaO}-\text{SiO}_2$  slag was produced as byproducts. Kinetic analysis indicates that silicon diffusion in slag is the rate-determining step of the reaction process. The reaction rate constant is around  $1.0 \times 10^{-4}$  s, and the effective diffusion film thickness in slag side is around  $10^{-3}$  cm at the silicon–slag interface. Slag basicity is suggested to increase to 1.31 for a faster silicon diffusion and further promotion of the reaction rate.

**KEYWORDS:** Recycling, Photovoltaic, Solar cells, Titanium silicides, Kinetic analysis

## INTRODUCTION

The rapid growth of the photovoltaic (PV) cell industry in recent years has resulted in large amount of silicon cutting kerf loss,<sup>1</sup> off-spec silicon,<sup>2</sup> and end-of-life PV cells.<sup>3,4</sup> If a good solution for recycling is developed, a huge accumulation of these silicon wastes can be avoided. However, a recent report in the industrial PV module recycling<sup>5</sup> shows the cost of Si wafers produced from recycled waste Si to be about 0.215 euro per wafer, and the cost for the collection of the waste Si is not included yet. Compared with the continuous price decline of the Si wafers used in the PV industry,<sup>6</sup> the recycled Si wafers do not show obvious advantages. A recycling method that is out of the loop of silicon reuse within the PV cell industry and able to assign some high added value to the products, such as titanium silicide, is in need as a promising supplement to the traditional silicon recycling processes.

Another continuously increasing solid waste is from the ironmaking industry. Ilmenite is one of the principal titanium minerals (95%) in the world but with limited utilization.<sup>7</sup> As a part of an important ironmaking process in China, titanium is

concentrated from ilmenite to titanium-bearing slag. For instance, Pangang Group Steel Co. produces more than 3 million tonnes/year of titanium-bearing blast furnace slag, which contains 22 to 25 wt %  $\text{TiO}_2$ .<sup>8</sup> Several technologies were invented to reutilize this resource.<sup>9–12</sup> The core task is recovery of titanium compounds from slag. However, the slag cannot be efficiently utilized, and the titanium is difficult to recover.<sup>13,14</sup>

The process introduced in the present work shows a great potential in recycling these two important solid wastes generated from the PV cell industry and ironmaking industry. The products with this recycling process, titanium silicides, are generally referred to  $\text{Ti}_5\text{Si}_3$  and  $\text{TiSi}_2$ , which have high added value. They are outstanding high-temperature materials<sup>15–17</sup> and can serve as a promising component of complementary metal-oxide semiconductor (CMOS)<sup>18</sup> and anodes for batteries.<sup>19–21</sup> Usually,

**Received:** February 27, 2018

**Revised:** March 27, 2018

**Published:** March 31, 2018

Table 1. Compositions and Weights of Slags Used in Experiments<sup>a</sup>

Temp./K	No.	Slag Composition/wt %			Basicity	Liquidus Temperature/K	Density of Slag/g cm <sup>-3</sup>	Viscosity of Slag/mPa s	Optical Basicity
		CaO	SiO <sub>2</sub>	TiO <sub>2</sub>					
1773	1	23	37	40	0.62	1693.15	2895	379	0.72
	2	26	34	40	0.76	1653.15	2910	238	0.74
	3	29	31	40	0.94	1657.15	2923	165	0.75
	4	32	28	40	1.14	1701.15	2934	125	0.77
	5	34	26	40	1.31	1762.15	2941	108	0.78

<sup>a</sup>Experiments at different reaction times are in progress.

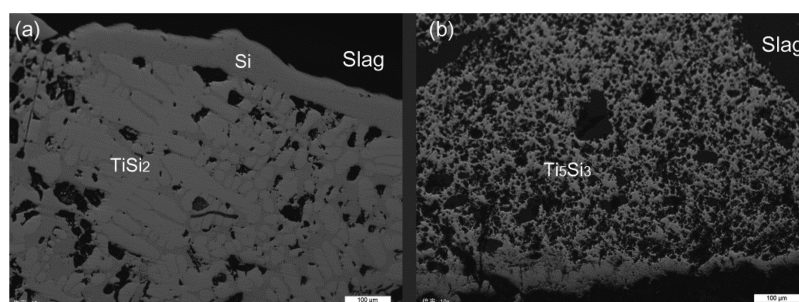


Figure 1. Optical microscope pictures of sample 5 after reaction for (a) 0.5 h and (b) 3 h at 1773 K.

they are prepared by solid state reaction from pure titanium and silicon powders.<sup>21,22</sup> High raw material costs of this method leads to a pricy product and limits its application. Recently, we reported an economical process to produce Ti<sub>5</sub>Si<sub>3</sub> from silicon and slag,<sup>23,24</sup> which has gained attention of other researchers. Zhang and Wang<sup>25</sup> successfully prepared Ti<sub>5</sub>Si<sub>3</sub> from actual blast furnace slag with 28 mass% TiO<sub>2</sub> for the first time. Although the previous reports only focused on slag recovery, we also proposed this method as a promising silicon recycling process to produce advanced materials. In the present work, the mechanism of this novel production method of Ti<sub>5</sub>Si<sub>3</sub> and TiSi<sub>2</sub> from titanium-bearing slag was studied. The experiments were designed to optimize the reaction kinetics for this feasible production process.

## MATERIALS AND METHODS

**Methods.** The industrial design of the process was a three-layered reaction process. Molten silicon floats on the surface of slag, and the heavy titanium silicide droplets precipitate through slag, deposit on the bottom of the reactor, and form a layer of titanium silicide. Reaction occurs at the interfaces of silicon–slag and falling droplets–slag. Although the three-layered reaction process could accelerate reaction rate and refine the product, accurate measurement of the reaction interface area becomes a problem in kinetic analysis. In this study, the initial position of slag and silicon was exchanged, i.e., slag maintains on the molten silicon, to obtain a stable reaction interface and hence simplify the kinetic analysis.

**Materials.** As a basic system of titanium-bearing blast furnace slag, TiO<sub>2</sub>–CaO–SiO<sub>2</sub> ternary (5 g) with different compositions was premelted at 1773 K from reagent-grade TiO<sub>2</sub>, SiO<sub>2</sub>, and CaO and reacted with 1 g of pure semiconductor grade silicon melt. CaO was calcined from CaCO<sub>3</sub> at 1273 K for 10 h in air. Raw materials which were placed in a high-purity graphite crucible (8 mm inner diameter) reacted at 1773 K inside a vertical tube furnace. The reaction time ranged from 0.2 to 20 h. Argon was introduced into the furnace during the reduction. The reaction condition is listed in Table 1. Basicity in Table 1 is defined as the weight ratio of CaO to SiO<sub>2</sub> in accordance with industrial practice. While optical basicity is one of the most important parameters of slag/glass for correlating trends of slag properties, in order to confirm the basicity trends of slag with TiO<sub>2</sub>, optical basicity was calculated based on the recommended values in the report of ref 26 as a function of the

polarizability of oxygen and cations. Specifically, the optical basicity of TiO<sub>2</sub> is the average value from refractive index and energy gap or glass refractivity and oxide refractive index. The optical basicity of slag increases from 0.72 to 0.78 with the increasing number of slag samples in Table 1. The density of slag is estimated using Mills' model<sup>27</sup> combining with the calculation results of the liquidus temperature of the slag via FactSage 7.0. Slag was put above the molten silicon in the experiments. Considering the density difference between slag and silicon, one could find that the density of slag is larger than that of liquid silicon (2.56 g cm<sup>-3</sup><sup>28</sup>). It is the relatively high viscosity of melts that kept a relatively stable position of the two phases.

**Characterization.** After the reaction, the sample was withdrawn from the furnace, quenched in argon gas, and subjected to characterization. The X-ray diffraction (XRD, Rigaku Rint-2100) analysis, optical microscopy, and scanning electron microscopy (JSM-6510LA, JEOL Ltd.) equipped with energy-dispersive spectroscopy (SEM/EDS) observations were conducted on the reaction products. Moreover, in order to quantitatively study the kinetics, inductively coupled plasma atomic emission spectroscopy (ICP-AES, SPS 7700, SII Nano Technology, Japan) was employed to analyze the composition of the quenched slag. For ICP-AES analysis, 0.5 g of Na<sub>2</sub>CO<sub>3</sub> and 0.5 g of Na<sub>2</sub>B<sub>4</sub>O<sub>7</sub> were used for digestion of 0.1 g of crushed slag in a Pt crucible at 1273.15 K for 20 min. Then, the alkaline-fused sample was dissolved in 1:3 HCl:H<sub>2</sub>O acid solution. The accuracy of this method has been approved by detection of the original slag before reaction. Calcium concentration in titanium silicides was detected by an electron probe microanalyzer (EPMA, JXA-8900R SuperProbe).

## RESULTS

**Reaction Products.** During the reaction, products, mainly containing Si, TiSi<sub>2</sub>, and Ti<sub>5</sub>Si<sub>3</sub>, were concentrated in the alloy part under slag. The reacted samples after reaction were investigated with an optical microscope. The pictures of sample 5 are shown in Figure 1. It shows that within 0.5 h well-developed dendritic TiSi<sub>2</sub> fills in the silicon matrix. Since the density of TiSi<sub>2</sub> is larger than that of molten silicon, a silicon layer exists between TiSi<sub>2</sub> bulk and slag. Prolonging the reaction time, TiSi<sub>2</sub> and molten Si transformed into Ti<sub>5</sub>Si<sub>3</sub>. During the process, silicon was transformed into a Ti solution with low Ti content, and then, the TiSi<sub>2</sub> phase formed. Ti<sub>5</sub>Si<sub>3</sub> was the final product if there was enough titanium in the reactor. Therefore, in the titanium

silicides synthesis, three reactions were employed: reduction of  $\text{TiO}_2$  to silicon dissolved titanium, synthetic reaction of the  $\text{TiSi}_2$  phase, and precipitation of  $\text{Ti}_5\text{Si}_3$ . Because CaO was contained in the reaction system, Ca could dissolve into the silicides. Teixeira et al.<sup>29</sup> reported that the concentration of Ca in molten silicon is 1.3 mass% in equilibrium with slag ( $\text{CaO}/\text{SiO}_2 = 1.21$ ). Due to the very limited Ca concentration in molten silicon and titanium silicides, we cannot observe Ca peaks in the EDS spectrum of the alloy samples. Moreover, the EMPA analysis results show that the Ca concentration in  $\text{TiSi}_2$  is from 0.23–0.30 mass%, and the Ca concentration in  $\text{Ti}_5\text{Si}_3$  is 0.01 mass%.

The composition change of the alloy part in the reaction was studied by XRD (Figures 2 and 3). Figure 2 shows the XRD

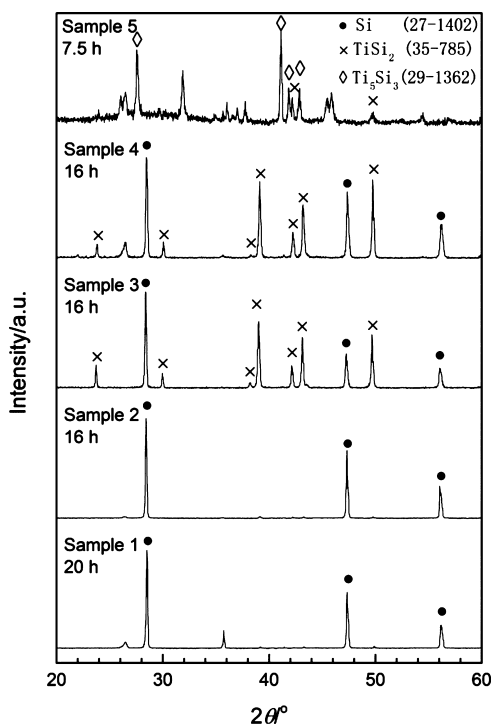


**Figure 2.** XRD spectrum of final products in all the quenched samples after reaction at 1773 K (unmarked peaks come from crystallized slag).

spectrum of the final products in the experiments. Samples 1 and 2 mainly contained silicon. The principal compositions are  $\text{TiSi}_2$  and Si in samples 1 and 2. A porous intermetallic bulk of  $\text{Ti}_5\text{Si}_3$  had been synthesized in sample 5. The unmarked peaks are attributed to trapped slag particles in  $\text{Ti}_5\text{Si}_3$ . Based on the results, one could conclude that titanium content in the silicon-based phases increases with the increasing slag basicity.

The XRD spectra of the alloy part of the samples quenched at different times are shown in Figure 3. As shown in Figure 3, the amount of  $\text{TiSi}_2$  increased with reaction time. One could notice that titanium silicides are hard to observe by XRD in some reacted samples as shown in both Figures 2 and 3. Therefore, SEM/EDS were employed to observe the cross section of the alloy part in the samples (Figure 4).  $\text{TiSi}_2$  crystals were detected at the grain boundary of the solidified silicon crystals in samples 1 and 2. The area fraction of  $\text{TiSi}_2$  precipitates increased with slag basicity. When the slag basicity increased to 1.31,  $\text{Ti}_5\text{Si}_3$  formed within 3 h.

All the obtained experimental results implied that although the prolonged reaction time could promote the formation of titanium silicide, slag basicity is the key point to accelerate the

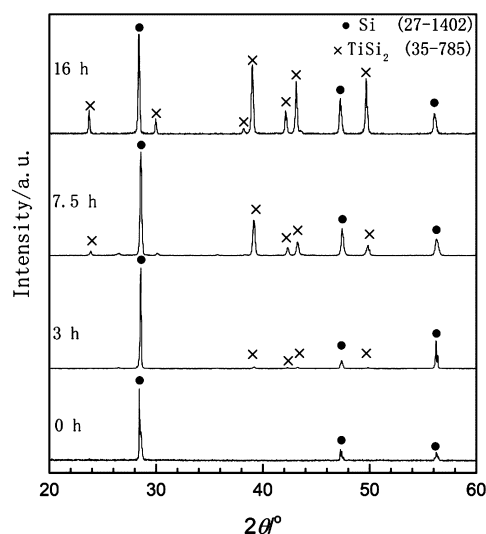
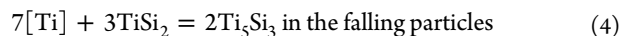
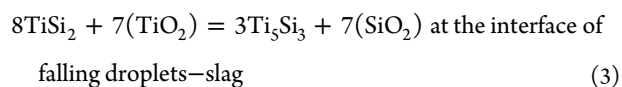
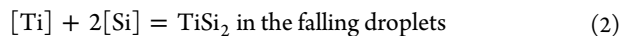
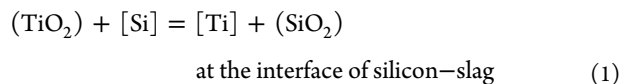


**Figure 3.** XRD spectrum of final products in quenched sample 3 after different reaction times at 1773 K (unmarked peaks come from crystallized slag).

reaction process. As an additional illustration, Figure 5 shows that the main product formed in sample 5 was  $\text{TiSi}_2$  after reaction for 0.5 h. The area fraction of  $\text{TiSi}_2$  in it is even higher than that in sample 1 after reaction for 6.5 h. Therefore, optimization of this synthesis process needs an investigation of the effect of slag basicity and the mechanism of the effect.

**Kinetic Mechanism.** Thermodynamic studies<sup>23,30,31</sup> verified that during the reduction of  $\text{TiO}_2$  to  $\text{Ti}_5\text{Si}_3$ ,  $\text{TiSi}_2$  forms as the reaction intermediate. If the silicon floats on slag as usual, the reaction occurs at the silicon–slag interface and in the slag, which is as follows:



Apparently, the reaction rate is relatively fast because abundant droplets in slag expand the reaction interface. Nevertheless, the number and sizes of the falling droplets vary with time and are hard to probe. Hence, estimation of the reaction interface area becomes a difficult statistical issue. As a result, the kinetic analysis is very difficult.

Therefore, an experimental strategy was applied in this work to prevent formation of droplets in slag. In this study, slag is stationed on the top of molten silicon (Figure 6). Although the density of slag is more than silicon, it still kept the same location after reaction in all the experiments because of the relatively high viscosity of melts. Due to this design, once the intermediate,  $\text{TiSi}_2$ , forms at the interface of the slag and silicon, it will fall to the bottom of the silicon, far away from the interface due to the density difference. The further reduction of titanium proceeds within silicon naturally. Figure 1(a) also supports this description of the reaction approach. Therefore, the reaction steps could be described as follows:

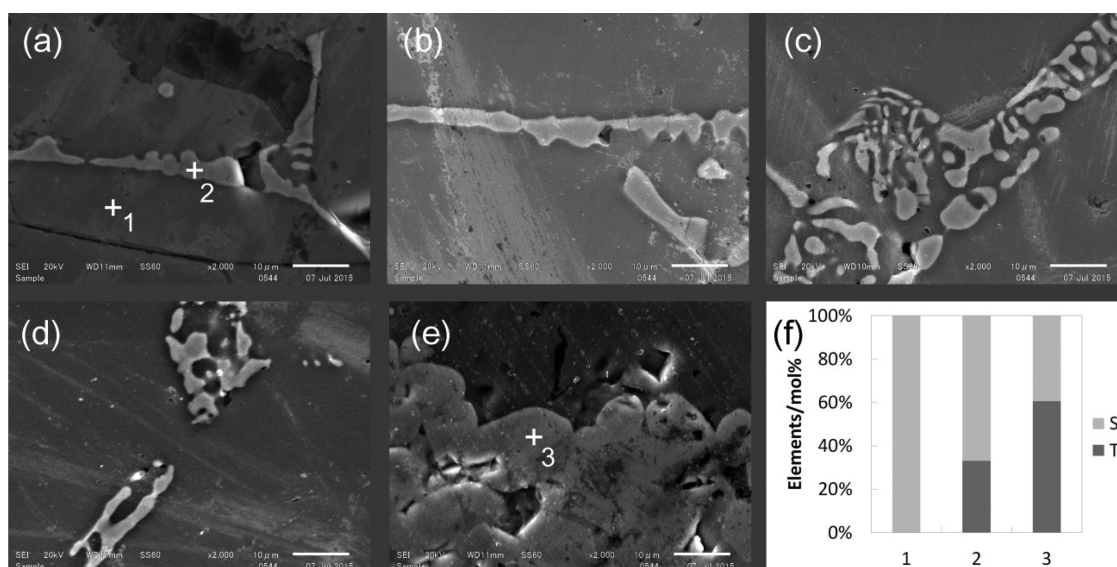


**Figure 4.** SEM and EDS results of products after reaction for 3 h at 1773 K: Microscopic photos of samples (a) No. 1, (b) No. 2, (c) No. 3, (d) No. 4, and (e) No. 5. (f) Elements' content of the three "+" points.

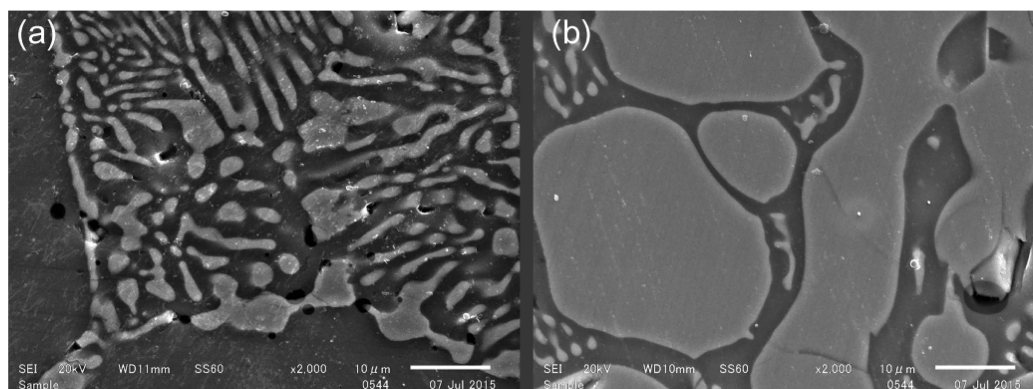


**Figure 5.** SEM photo of cross section: (a) Sample 1 after reaction for 6.5 h and (b) sample 5 after reaction for 0.5 h at 1773 K.

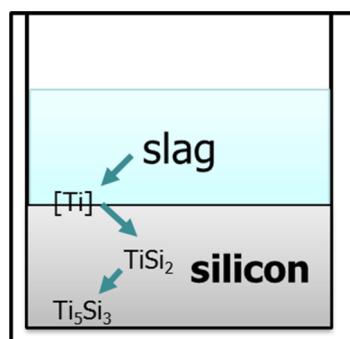
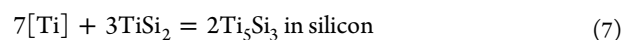
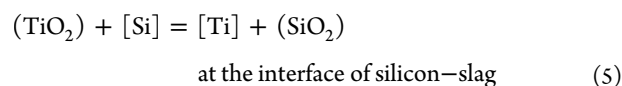


**Figure 6.** Illustration of the reaction in the experiments.



The reaction equilibrium constant of eq 5 is 2.88 at 1773 K, which indicates the ratio of reaction rate constants in the direction of forward and backward is small. Therefore, this

chemical reaction could be regarded as a reversible reaction.  $\text{TiSi}_2$  and  $\text{Ti}_5\text{Si}_3$  disperse in the silicon as liquid drops and solid particles, respectively. Therefore, the reaction interfaces of eqs 6 and 7 could be several times larger than the slag–silicon interface. It indicates that the chemical reaction rate of eqs 6 and 7 are too fast to be reaction rate-determining steps. Apparently, the reaction rate-determining step should be related to eq 5, which could be one of the following steps:

- (1) Diffusion of  $(\text{TiO}_2)$  through the slag phase to the slag–silicon interface
- (2) Diffusion of  $[\text{Si}]$  from silicon bulk to the slag–silicon interface
- (3) Chemical reaction producing  $[\text{Ti}]$  and  $(\text{SiO}_2)$  at the interface
- (4) Diffusion of  $[\text{Ti}]$  from the interface to silicon bulk phase
- (5) Diffusion of  $(\text{SiO}_2)$  from the interface to the slag bulk phase

If step 3 is an irreversible reaction, then steps 4 and 5 would not be the rate-determining steps. Equation 5, however, is a reversible reaction because of the relatively low Gibbs energy change of this reaction, i.e., low reaction equilibrium constant.<sup>23</sup> It implies that all the five steps could be the rate-determining step of the reaction process. It is well known that the diffusion in the molten silicon or metallic bulk phase is much quicker than the

diffusion in the slag bulk phase. Kubiček and Pepríca<sup>32</sup> suggested that diffusion of an element through liquid metal is approximately an order of magnitude faster than that of the same element through liquid slag. Therefore, only steps 1, 3, and 5 are possible to be the rate-determining steps.

**Kinetic Model.** The rate-determining step could be assumed to be the following:

1. Transport of (TiO<sub>2</sub>) in Slag Diffusion Layer.

$$\frac{dn_{\text{TiO}_2}}{dt} = Ak_{\text{TiO}_2}(x_{\text{TiO}_2}^i - x_{\text{TiO}_2}) \quad (8)$$

where  $n_{\text{TiO}_2}$  is the amount of TiO<sub>2</sub>;  $t$  is reaction time;  $A$  is the area of reaction interface, which is assumed to be constant (0.005 m<sup>2</sup>) in the reaction;  $k_{\text{TiO}_2}$  is the diffusion constant of TiO<sub>2</sub> from slag to the reaction interface;  $x_{\text{TiO}_2}^i$  and  $x_{\text{TiO}_2}$  are the mole fractions of TiO<sub>2</sub> at the interface and in the bulk phase of slag, respectively.

It should be noted that the chemical equilibrium constant of eq 5 is the following:

$$K_{(1)} = \frac{x_{(\text{SiO}_2)_i} x_{\text{Ti}}}{x_{(\text{TiO}_2)_i} x_{\text{Si}}} \quad (9)$$

where  $K_{(1)}$  is the equilibrium constant of eq 5;  $x_{(\text{SiO}_2)_i}$  is the mole fraction of SiO<sub>2</sub> at the interface;  $x_{\text{Ti}}$  and  $x_{\text{Si}}$  are the mole fractions of Ti and Si in molten silicon bulk phase, respectively, which satisfies

$$x_{\text{Ti}} + x_{\text{Si}} = 1 \quad (10)$$

Because the reaction rate of eq 6 was fast enough compared to eq 5, the reactants, [Ti] and [Si], are in equilibrium with TiSi<sub>2</sub>. In other words,  $\frac{x_{\text{Ti}}}{x_{\text{Si}}}$  is constant,  $u$ , which could be obtained from the equilibrium constant of eq 6

$$K_{(2)} = \frac{1}{x_{\text{Ti}}(x_{\text{Si}})^2} \quad (11)$$

where  $K_{(2)}$  is the equilibrium constant of eq 6 and is equal to  $2.81 \times 10^3$  at 1773 K. Therefore,

$$(1 + u)^3 - uK_{(2)} = 0 \quad (12)$$

The value of  $u$  was estimated to be  $5.3 \times 10^4$  at 1773 K using the Newton–Raphson method. Here,  $x_{(\text{CaO})_i}$  is a constant which is equal to  $x_{\text{CaO}}$ , thus

$$K_{(1)} = u \frac{1 - x_{\text{CaO}} - x_{(\text{TiO}_2)_i}}{x_{(\text{TiO}_2)_i}} \quad (13)$$

where  $x_{\text{CaO}}$  is the mole fraction of CaO in the bulk phase of slag. Based on eq 13, one could obtain

$$x_{(\text{TiO}_2)_i} = \frac{1 - x_{\text{CaO}}}{1 + K_{(1)}/u} \quad (14)$$

With eq 14, eq 8 turns out to be

$$\frac{dn_{\text{TiO}_2}}{dt} = Ak_{\text{TiO}_2} \left( \frac{1 - x_{\text{CaO}}}{1 + K_{(1)}/u} - x_{\text{TiO}_2} \right) \quad (15)$$

$$n_{\text{TiO}_2} = x_{\text{TiO}_2} n_{\text{slag}} \quad (16)$$

where  $n_{\text{slag}}$  is the amount of slag, which keeps constant during the reaction;  $\omega_{\text{TiO}_2}$  is the mass ratio of TiO<sub>2</sub> in the slag.

Combining eqs 15 and 16

$$\frac{dx_{\text{TiO}_2}}{dt} = \frac{A}{n_{\text{slag}}} k_{\text{TiO}_2} \left( \frac{1 - x_{\text{CaO}}}{1 + K_{(1)}/u} - x_{\text{TiO}_2} \right) \quad (17)$$

in the term of integration

$$\ln \frac{x_{\text{TiO}_2} - a_1}{x_{(\text{TiO}_2)_0} - a_1} = -\frac{A}{n_{\text{slag}}} k_{\text{TiO}_2} t \quad (18)$$

where

$$a_1 = \frac{1 - x_{\text{CaO}}}{1 + K_{(1)}/u} \quad (19)$$

2. Transport of (SiO<sub>2</sub>) in Slag Diffusion Layer. Similar to the transport of TiO<sub>2</sub> in the slag diffusion layer, one could get

$$\frac{dx_{\text{SiO}_2}}{dt} = \frac{A}{n_{\text{slag}}} k_{\text{SiO}_2} (x_{(\text{SiO}_2)_i} - x_{\text{SiO}_2}) \quad (20)$$

where  $k_{\text{SiO}_2}$  is the diffusion constant of SiO<sub>2</sub> from slag to the reaction interface;  $x_{\text{SiO}_2}$  is the mole fraction of SiO<sub>2</sub> in the bulk phase of slag, which meets the relationship of

$$x_{\text{SiO}_2} = 1 - x_{\text{CaO}} - x_{\text{TiO}_2} \quad (21)$$

Considering that  $x_{(\text{CaO})_i}$  in eq 20 is a constant which is equal to  $x_{\text{CaO}}$ , based on eq 14, one obtains

$$x_{(\text{SiO}_2)_i} = \frac{K_{(1)}(1 - x_{\text{CaO}})}{u + K_{(1)}} \quad (22)$$

Likewise, the reaction kinetics in the term of integration

$$\ln \frac{x_{\text{TiO}_2} - a_2}{x_{(\text{TiO}_2)_0} - a_2} = -\frac{A}{n_{\text{slag}}} k_{\text{SiO}_2} t \quad (23)$$

where

$$a_2 = \frac{(1 - x_{\text{CaO}})K_{(1)}}{u + K_{(1)}} \quad (24)$$

3. Interfacial Reaction. The interface reaction was assumed to be a first-order reversible chemical reaction, and it should be noticed that the concentration at the interface is equal to the concentration within bulk phase

$$-\frac{dx_{\text{TiO}_2}}{dt} = \frac{A}{n_{\text{slag}}} (k_+ x_{\text{TiO}_2} - k_- x_{\text{SiO}_2}) \quad (25)$$

where  $k_+$  and  $k_-$  represent the rate constant for the chemical reaction in eq 5 in the direction of forward and backward, respectively

$$K_{(1)} = k_+/k_- \quad (26)$$

Therefore, eq 25 turns out to be

$$\frac{dx_{\text{TiO}_2}}{dt} = \frac{A}{n_{\text{slag}}} \frac{K_{(1)} + 1}{K_{(1)}} k_+ \left[ \frac{1}{K_{(1)} + 1} (1 - x_{\text{CaO}}) - x_{\text{TiO}_2} \right] \quad (27)$$

in the term of integration

$$\ln \frac{x_{\text{TiO}_2} - a_3}{x_{(\text{TiO}_2)_0} - a_3} = -\frac{(1 + K_{(1)})A}{K_{(1)}n_{\text{slag}}} k_+ t \quad (28)$$

where

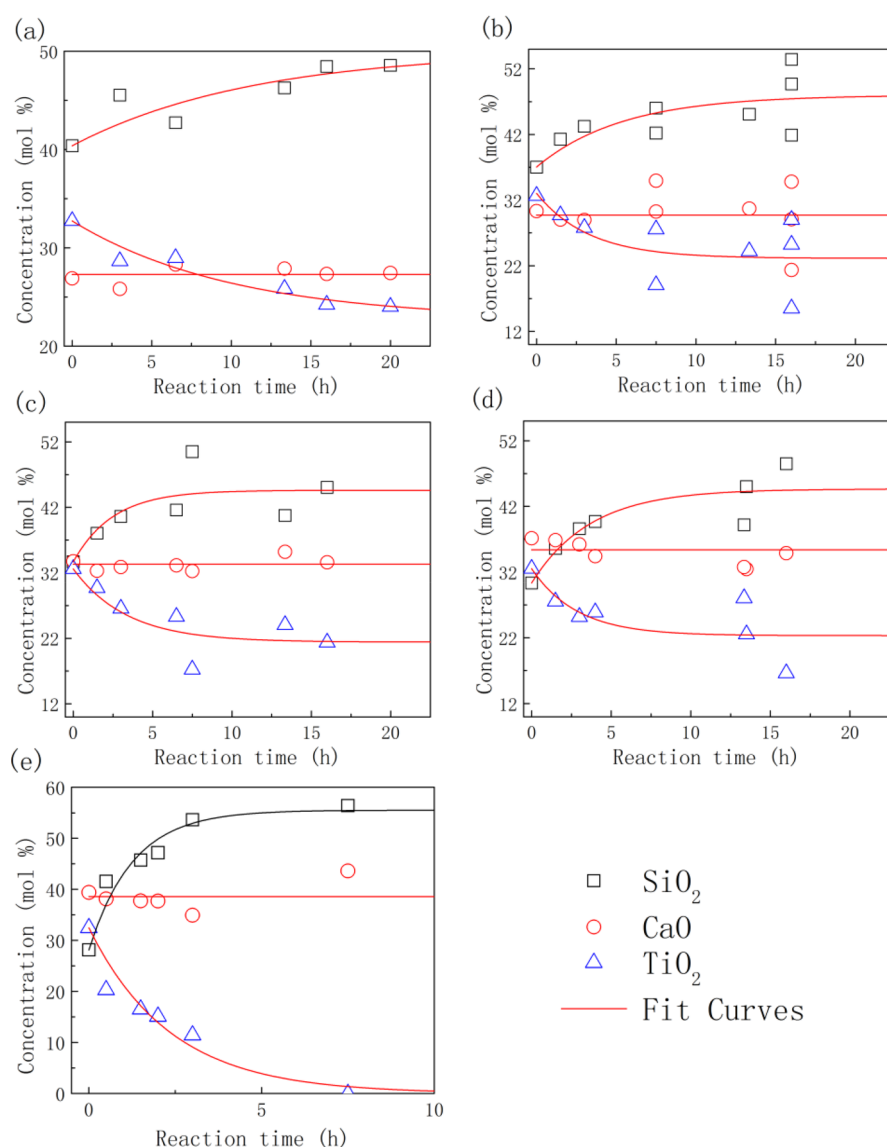


**Figure 7.** Relationship of slag composition in the reaction of titanium-bearing slag with molten silicon at 1773 K in Ar atmosphere: (a) No. 1, (b) No. 2, (c) No. 3, (d) No. 4, and (e) No. 5 (fit curves are the fitting results of eq 30).

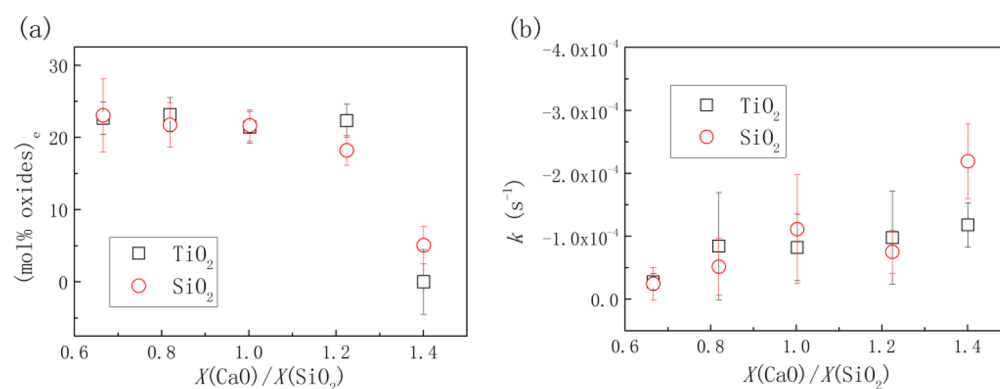


**Figure 8.** Kinetic parameters in eq 30 to describe the reaction of titanium-bearing slag with molten silicon at 1773 K in Ar atmosphere: (a) Final concentration (mol %TiO<sub>2</sub>)<sub>e</sub> and (b) reaction rate constant  $k$ .

$$a_3 = \frac{1 - x_{\text{CaO}}}{K_{(1)} + 1} \quad (29)$$

It could be noticed that kinetic models of eqs 18, 23, and 28 are similar. At high temperature, diffusion is always the rate-determining step. A kinetic analysis based on experimental data could be used to investigate the reaction mechanism.

**Reaction Kinetics.** The isothermal kinetic model of eqs 18, 23, and 28 could be presented as follows:

$$\ln \frac{(\text{mol}\% \text{TiO}_2)_e - (\text{mol}\% \text{TiO}_2)_0}{(\text{mol}\% \text{TiO}_2)_e} = -kt \quad (30)$$

where (mol %TiO<sub>2</sub>) is the molar percentage of TiO<sub>2</sub> in slag; subscripts 0 and e represent the initial and final state of the reaction, respectively; *k* represents the apparent reaction rate constant; *t* represents the reaction time. This kinetic model could be used to describe the reaction with a rate-determining step as one of the before mentioned three steps. The only difference among the mechanisms is that the parameters *a*<sub>1</sub>, *a*<sub>2</sub>, and *a*<sub>3</sub> which could be calculated from theory were replaced to be an empirical value which was obtained from the experiments.

Equation 30 was used to fit the ICP results of the slag composition after the reaction. As shown in Figure 7, the extraction rate of TiO<sub>2</sub> from slag was the fastest at the beginning, and it decreased with reaction time. The TiO<sub>2</sub> concentration in slag could achieve the lowest point within 15 h when the slag basicity is higher than 0.62. Moreover, TiO<sub>2</sub> content in the stable state decreased with increasing slag basicity. When the basicity rose to 1.31, almost all TiO<sub>2</sub> in the slag could be extracted out. The fitted kinetic parameters in Figure 8 could also show these trends. Figure 8 shows that the reaction rate constant is around 10<sup>-4</sup> s<sup>-1</sup>. It is known that

$$k = -\frac{A}{V_{\text{slag}}} \frac{D}{\delta} \quad (31)$$

where *V*<sub>slag</sub> is the volume of slag; *D* is the diffusion coefficient of silicon in slag; *δ* represents effective film thickness. Nagata and Goto<sup>33</sup> suggested that the diffusion constant of silicon in a CaO–SiO<sub>2</sub>–Al<sub>2</sub>O<sub>3</sub> slag at 1773 K was 2.3 × 10<sup>-7</sup> cm<sup>2</sup> s<sup>-1</sup> based on the report of Towers and Chipman.<sup>34</sup> Based on the reported data, it could be estimated that the effective film thickness is around 10<sup>-3</sup> cm. This result corresponds well with the EDS result of the cross section of the quenched sample in Figure 9.

Moreover, Figure 8 suggests that silica was produced as a byproduct when synthesizing titanium silicide. Silica dissolved into slag, forming a CaO–SiO<sub>2</sub> binary. Titanium-free blast furnace slag has been extensively used for road making and in the cement industry. Specifically, the air-cooled slag has been fully

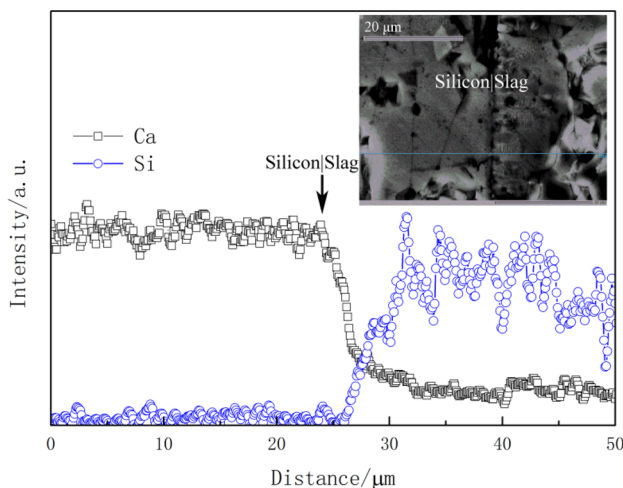


**Figure 9.** EDS result: Silicon intensity at the slag–silicon interface in the quenched sample 1 after reaction for 3 h.

utilized globally.<sup>35</sup> Therefore, all the wastes can be effectively transformed into commercial products in an optimized condition.

## DISCUSSION

If the rate-determining step of the reaction is the mass transfer of (TiO<sub>2</sub>) from the slag bulk phase to the slag–silicon interface, the reaction rate could be represented by the diffusion rate of (TiO<sub>2</sub>) as shown by eq 8. The initial reaction rate (*dx*<sub>TiO<sub>2</sub></sub>/*dt*)<sub>0</sub> will be

$$\left( \frac{dx_{\text{TiO}_2}}{dt} \right)_0 = -\frac{A}{n_{\text{slag}}} k_{\text{TiO}_2} x_{\text{TiO}_2}^0 = \text{cons.} \quad (32)$$

where *A* is the area of reaction interface which is equal to the inner area of graphite crucible; *k*<sub>TiO<sub>2</sub></sub> is the rate constant of diffusion step; *x*<sub>TiO<sub>2</sub></sub><sup>0</sup> represents the initial concentration of TiO<sub>2</sub> in the bulk phase. The initial TiO<sub>2</sub> content in the slag was fixed in all experiments. According to eq 32, the initial reaction rate should be same in this experimental work. However, Figure 7 shows that the initial reaction rate, the slope of the TiO<sub>2</sub> concentration profiles at the beginning, varies with slag composition. It indicates that the reaction rate is not determined by the diffusion of titanium in slag.

If one assume that the interfacial chemical reaction was the rate-determining step, the value of the initial reaction rate should match eq 27

$$\left( \frac{dx_{\text{TiO}_2}}{dt} \right)_0 = \frac{A}{n_{\text{slag}}} \frac{K_{(1)} + 1}{K_{(1)}} k_{\text{t}} \left[ \frac{1}{K_{(1)} + 1} (1 - x_{\text{CaO}}) - x_{\text{TiO}_2}^0 \right] = \text{cons.} \quad (33)$$

Correspondingly, with the same TiO<sub>2</sub> concentration in slag and the same pure silicon as reactants, the initial reaction rates of every experiment should be the same. Therefore, only step 5, diffusion of SiO<sub>2</sub> from the interface to the slag bulk phase, could be the rate-determining step in this reaction. The experimental study of Dolan and Johnston<sup>36</sup> indicated that the diffusion coefficient of silicon increased with increasing optical basicity. It confirms that the accelerated reaction rate with the high basicity slag corresponds to the improved diffusion rate of SiO<sub>2</sub>.

## CONCLUSIONS

Titanium silicides were produced in the reduction process of molten silicon at 1773 K with TiO<sub>2</sub>–CaO–SiO<sub>2</sub> slag as reductant. TiSi<sub>2</sub> was obtained with slag basicity higher than 0.62. Ti<sub>5</sub>Si<sub>3</sub> could be produced within 3 h with slag basicity of 1.31. CaO–SiO<sub>2</sub> slag was produced as byproducts for road making or cement manufacture. The result shows this process is promising in silicon waste and steelmaking slag recovery.

Reaction mechanism of this process is discussed and based on the three-step reaction mechanism: TiO<sub>2</sub> → TiSi<sub>2</sub> → Ti<sub>5</sub>Si<sub>3</sub>. Experiments are designed to quantitatively study kinetics of the reaction. The kinetic model of

$$\ln \frac{(\text{mol}\% \text{TiO}_2)_e - (\text{mol}\% \text{TiO}_2)_0}{(\text{mol}\% \text{TiO}_2)_e} = -kt$$

is summarized from different conditions and employed to the kinetic analysis. As a result, diffusion of silicon from the silicon–slag interface to the slag bulk is recommended as the rate-

determining step. The effective diffusion film thickness in slag side is estimated to be around  $10^{-3}$  cm. The reaction rate constant is around  $1.0 \times 10^{-4}$  s and increases with increasing slag basicity. Therefore, elevating slag basicity can promote recovery efficiency of silicon and titanium in this process.

## AUTHOR INFORMATION

### Corresponding Author

\* E-mail: [aha\\_c@126.com](mailto:aha_c@126.com). Tel: +31 (0)15 27 82307.

### ORCID

Zhiyuan Chen: 0000-0002-7993-7386

### Funding

This research did not receive any specific grant from funding agencies in the public, commercial, or not-for-profit sectors.

### Notes

The authors declare no competing financial interest.

## ACKNOWLEDGMENTS

The main work of this research was carried out at The University of Tokyo. Zhiyuan Chen and Yuliu You formerly worked at the University of Tokyo and now work at TU Delft. The authors express our thanks to Ir. Kees Kwakernaak and Prof. Yongxiang Yang from TU Delft for their technical and financial contributions of EPMA analysis, respectively.

## REFERENCES

- (1) Wang, T. Y.; Lin, Y. C.; Tai, C. Y.; Sivakumar, R.; Rai, D. K.; Lan, C. W. A novel approach for recycling of kerf loss silicon from cutting slurry waste for solar cell applications. *J. Cryst. Growth* **2008**, *310*, 3403–3406.
- (2) Woditsch, P.; Koch, W. Solar grade silicon feedstock supply for PV industry. *Sol. Energy Mater. Sol. Cells* **2002**, *72*, 11–26.
- (3) Shin, J.; Park, J.; Park, N. A method to recycle silicon wafer from end-of-life photovoltaic module and solar panels by using recycled silicon wafers. *Sol. Energy Mater. Sol. Cells* **2017**, *162*, 1–6.
- (4) Paiano, A. Photovoltaic waste assessment in Italy. *Renewable Sustainable Energy Rev.* **2015**, *41*, 99–112.
- (5) McDonald, N. C.; Pearce, J. M. Producer responsibility and recycling solar photovoltaic modules. *Energy Policy* **2010**, *38*, 7041–7047.
- (6) Zhang, F.; Gallagher, K. S. Innovation and technology transfer through global value chains: Evidence from China's PV industry. *Energy Policy* **2016**, *94*, 191–203.
- (7) Sahu, K. K.; Alex, T. C.; Mishra, D.; Agrawal, A. An overview on the production of pigment grade titania from titania-rich slag. *Waste Manage. Res.* **2006**, *24*, 74–79.
- (8) Zhang, L.; Zhang, L. N.; Wang, M. Y.; Li, G. Q.; Sui, Z. T. Recovery of titanium compounds from molten Ti-bearing blast furnace slag under the dynamic oxidation condition. *Miner. Eng.* **2007**, *20*, 684–693.
- (9) Lou, T.; Li, Y.; Li, L.; Sui, Z. Study of precipitation of perovskite phase from the oxide slag. *Acta Metall. Sin.* **2000**, *36*, 141–144.
- (10) Liu, X.; Gai, G.; Yang, Y.; Sui, Z.; Li, L.; Fu, J. Kinetics of the leaching of  $TiO_2$  from Ti-bearing blast furnace slag. *J. China Univ. Min. Technol.* **2008**, *18*, 275–278.
- (11) Huang, Z.; Wang, M.; Du, X.; Sui, Z. Recovery of titanium from the rich titanium slag by  $H_2SO_4$  method. *J. Mater. Sci. Technol.* **2003**, *19*, 191–192.
- (12) Wang, M.; Li, L.; Zhang, L.; Zhang, L.; Tu, G.; Sui, Z. Effect of oxidation on enrichment behavior of  $TiO_2$  in titanium-bearing slag. *Rare Met.* **2006**, *25*, 106–110.
- (13) He-gui, D. *Theory of Smelting V and Ti-Magnetite by Blast Furnace*; Science Press, Beijing, 1996.
- (14) Valighazvini, F.; Rashchi, F.; Khayyam Nekouei, R. Recovery of Titanium from Blast Furnace Slag. *Ind. Eng. Chem. Res.* **2013**, *52*, 1723–1730.

(15) Zhang, L.; Wu, J.  $Ti_5Si_3$  and  $Ti_3Si_2$ -based alloys: Alloying behavior, microstructure and mechanical property evaluation. *Acta Mater.* **1998**, *46*, 3535–3546.

(16) Frommeyer, G.; Rosenkranz, R. In *Metallic Materials with High Structural Efficiency*; Senkov, O., Miracle, D., Firstov, S., Eds.; Springer: The Netherlands, 2004; Vol. 146, Chapter 30, pp 287–308, DOI 10.1007/1-4020-2112-7\_30.

(17) Mitra, R. Microstructure and mechanical behavior of reaction hot-pressed titanium silicide and titanium silicide-based alloys and composites. *Metall. Mater. Trans. A* **1998**, *29*, 1629–1641.

(18) Frank, M. M.; Cabral, C.; Dechene, J. M.; Orttoland, C.; Zhu, Y.; Marshall, E. D.; Murray, C. E.; Chudzik, M. P. Titanium Silicide/Titanium Nitride Full Metal Gates for Dual-Channel Gate-First CMOS. *IEEE Electron Device Lett.* **2016**, *37*, 150–153.

(19) Wang, Y. H.; He, Y.; Xiao, R. J.; Li, H.; Aifantis, K. E.; Huang, X. J. Investigation of crack patterns and cyclic performance of Ti–Si nanocomposite thin film anodes for lithium ion batteries. *J. Power Sources* **2012**, *202*, 236–245.

(20) Wang, X.; Wen, Z.; Liu, Y.; Huang, L.; Wu, M. Study on Si–Ti alloy dispersed in a glassy matrix as an anode material for lithium-ion batteries. *J. Alloys Compd.* **2010**, *506*, 317–322.

(21) Lee, Y. S.; Lee, J. H.; Kim, Y. W.; Sun, Y. K.; Lee, S. M. Rapidly solidified Ti–Si alloys/carbon composites as anode for Li-ion batteries. *Electrochim. Acta* **2006**, *52*, 1523–1526.

(22) Tang, Z.; Thom, A. J.; Akinc, M. Role of nitrogen on the oxidative stability of  $Ti_3Si_2$  based alloys at elevated temperature. *Intermetallics* **2006**, *14*, 537–543.

(23) Chen, Z.; Li, Y.; Tan, Y.; Morita, K. Reduction of Titanium Oxide by Molten Silicon to Synthesize Titanium Silicide. *Mater. Trans.* **2015**, *56*, 1919–1922.

(24) Chen, Z.; Morita, K. *Reduction of Titanium Bearing Slag to Titanium Silicide*; Presented at the 170th ISIJ Conference, Fukuoka, Japan, September 2015.

(25) Zhang, G.-H.; Wang, K.-F. Preparation of  $Ti_5Si_3$  by silicothermic reduction of titanium-bearing blast furnace slag. *Can. Metall. Q.* **2018**, *57*, 80–88.

(26) Rodriguez, C. P.; McCloy, J.; Schweiger, M.; Crum, J. V.; Winschell, A. *Optical Basicity and Nepheline Crystallization in High Alumina Glasses*; Pacific Northwest National Laboratory, Richland, WA, 2011; DOI 10.2172/1019213.

(27) Mills, K.; Yuan, L.; Jones, R. Estimating the physical properties of slags. *J. S. Afr. Inst. Min. Metall.* **2011**, *111*, 649–658.

(28) Sasaki, H.; Tokizaki, E.; Terashima, K.; Kimura, S. Density variation of molten silicon measured by an improved Archimedian method. *Jpn. J. Appl. Phys.* **1994**, *33*, 3803.

(29) Teixeira, L. A. V.; Tokuda, Y.; Yoko, T.; Morita, K. Behavior and state of boron in CaO– $SiO_2$  slags during refining of solar grade silicon. *ISIJ Int.* **2009**, *49*, 777–782.

(30) Chushao, Xu; Liu, T. The smelting processes of ferroalloys using the titanium-bearing slags from blast furnaces (in Chinese). *Min. Metall. Eng.* **1988**, *8*, 41–45.

(31) Zushu, Li; Xu, C. Thermodynamics of smelting process of ferroalloys by silicothermic reduction of titanium-bearing slag (in Chinese). *Sichuan Metall.* **1993**, *25*, 74–77.

(32) Kubiček, P.; Pepríca, T. Diffusion in molten metals and melts: application to diffusion in molten iron. *Int. Met. Rev.* **1983**, *28*, 131–157.

(33) Nagata, K.; Goto, K. Transport Coefficients of Ions and Interdiffusivities in Multicomponent Ionic Solution of CaO– $SiO_2$ – $Al_2O_3$  at 1500° C. *J. Electrochem. Soc.* **1976**, *123*, 1814–1820.

(34) Towers, H.; Chipman, J. Diffusion of calcium and silicon in a lime-alumina-silica slag. *JOM* **1957**, *9*, 769–773.

(35) Das, B.; Prakash, S.; Reddy, P. S. R.; Misra, V. N. An overview of utilization of slag and sludge from steel industries. *Resources, Conservation and Recycling* **2007**, *50*, 40–57.

(36) Dolan, M. D.; Johnston, R. Multicomponent diffusion in molten slags. *Metall. Mater. Trans. B* **2004**, *35*, 675–684.